Accepted Manuscript

Study on heterogeneous photocatalytic ozonation degradation of ciprofloxacin by TiO_2/carbon dots: Kinetic, mechanism and pathway investigation

Yongqin Zeng, Danni Chen, Tiansheng Chen, Meixuan Cai, Qianxin Zhang, Zhijie Xie, Ruobai Li, Zhenjun Xiao, Guoguang Liu, Wenying Lv

PII: S0045-6535(19)30686-1

DOI: https://doi.org/10.1016/j.chemosphere.2019.04.039

Reference: CHEM 23547

To appear in: *ECSN*

Received Date: 23 November 2018

Revised Date: 5 March 2019

Accepted Date: 6 April 2019

Please cite this article as: Zeng, Y., Chen, D., Chen, T., Cai, M., Zhang, Q., Xie, Z., Li, R., Xiao, Z., Liu, G., Lv, W., Study on heterogeneous photocatalytic ozonation degradation of ciprofloxacin by TiO_2/carbon dots: Kinetic, mechanism and pathway investigation, *Chemosphere* (2019), doi: https://doi.org/10.1016/j.chemosphere.2019.04.039.

Study on heterogeneous photocatalytic ozonation degradation of ciprofloxacin by TiO_2/carbon dots: kinetic, mechanism and pathway investigation

Yongqin Zeng[a], Danni Chen[a], Tiansheng Chen[a], Meixuan Cai[a], Qianxin Zhang[a], Zhijie Xie[a], Ruobai Li[a], Zhenjun Xiao[a], Guoguang Liu[a]*, Wenying Lv[a]*

[a]School of Environmental Science and Engineering, Institute of Environmental Health and Pollution Control, Guangdong University of Technology, Guangzhou, 510006, China

* **Corresponding Author**: Guoguang Liu, Wenying Lv

E-mail: liugg615@163.com; lvwy612@163.com

Telephone: +86-20-39322547

Fax: +86-20-39322548

Address: School of Environmental Science and Engineering，Guangdong University of Technology, No. 100 Waihuan Xi Road, Guangzhou Higher Education Mega Center, Guangzhou, P.R China, Post Code: 510006

Abstract

In this study, the objective was mainly focusing on the mechanism investigation of ciprofloxacin (CIP) degradation by photocatalytic ozonation process which carried out by ozone and TiO_2 with a low content of carbon-dots (CDs) under simulated sunlight irradiation. The physicochemical properties of the prepared photocatalysts were characterized by X-ray diffraction (XRD), transmission electron microscopy (TEM), scanning electron microscope (SEM) X-ray photoelectron spectroscopy (XPS) and zeta potential. Comprehensive investigation has proven the process to be efficient in the removal of CIP with high yield of reactive species (•OH, $O_2^{\bullet-}$, h^+, etc.). Kinetic model on pH investigation found out a repulsive force between the photocatalysts and CIP intensified with the increasing pH, so did the production rate of hydroxyl radicals (•OH), while eventually reached a balance and achieved a maximum degradation rate. The results indicated that the enhancement mechanism was triggered by the photoexcited electron accumulated on CDs and transferred by ozone, resulting in the continuous generation of h+, $O_3^{\bullet-}$ and $O_2^{\bullet-}$. Possible photocatalytic ozonation degradation pathways of CIP were proposed according to the identifications of intermediates using high-resolution accurate-mass spectrometry (HRAM) LC-MS/MS.

Keywords: carbon-dots; ciprofloxacin; reactive species; photocatalytic ozonation; transformation pathway

1. Introduction

Pharmaceuticals and personal care products (PPCPs)，as "emerging contaminants", have received much attention in recent years (Zhang et al., 2018a). The occurrence of PPCPs was primarily attributed to the abuse in animal husbandry, industrial wastewater emissions, domestic water discharge, etc. Due to their persistent physicochemical properties and ineffectiveness to biodegradation, wastewater treatment plants have not always been efficient in the removal of PPCPs (Verlicchi et al., 2012). Consequently, multiple PPCPs have been detected in surface water, groundwater, and potable water. Ciprofloxacin (CIP), for example, a broad spectrum fluoroquinolone antibacterial agent, is effective in treating various infection(Zhou and Jiang, 2015). A total amount of 5340 tons of CIP was used in China in 2013, which was the second highest among all the fluoroquinolone antibiotics prescribed in China (Zhang et al., 2015). The concentration of CIP has been detected in hospital wastewater up to 21 μg/L, and in concentration up to several μg/L in secondary treated effluent due to the incomplete removal of conventional WWTPs (Doorslaer et al., 2014). Though CIP showed low toxic value on biological samples (Steenbergen et al., 2017), it is worth noticing that studies indicated that antibiotic resistant bacteria and resistance genes would be given birth by the effect of CIP at a low level (ng/L) (Erik et al., 2011; Rodriguez-Mozaz et al., 2015). In this case, genetic variants of microorganism will be threatened and adverse impact will be imposed on human health (Kümmerer, 2009; Kenny et al., 2012). In addition, the removal of PPCPs from wastewater can make a significant contribution to water conservation and

recirculation, which is achievement of sustainability.

Photocatalysis has been considerably studied in different contaminants treatment fields(Wen et al., 2016; Ye et al., 2018; Li et al., 2019). Titanium dioxide (TiO_2) is one of the promising photocatalysts which has been extensively investigated due to its high chemical stability, low cost, environmentally friendliness and optical properties (Wang et al., 2019). However, several disadvantages of pure TiO_2 such as the rapid recombination of photoexcited electron-holes pairs and exclusively activated with UV light ($\lambda \leq 380$ nm) might restrain the development of practical application. In this case, carbon dots (CDs) was considered to modify the photocatalytic performance of TiO_2. CDs possesses remarkable up-converted photoluminescence (PL) behavior, which indicates CDs could convert lower-energy light ($500 \leq \lambda \leq 1000$ nm) to high-energy light ($325 \leq \lambda \leq 425$ nm). In addition, with advantages of functional surface moieties, CDs could improve electron transferring and storing capacity. Indicating that CDs might have the ability to conduct as a promising component in photocatalysts modification (Fang et al., 2016; Martins et al., 2016). Thus, the composition of CDs on TiO_2 owned the ability to enhance light adsorption efficiency and photocatalytic performance by broadening the photo-absorption region and decreasing the recombination of electron-hole pairs(Wang et al., 2017b; Xie et al., 2018; Zhang et al., 2018b). According to our previous work, the synthesized CDs could avoid the recombination of holes and electrons by transferring the photogenerated electrons from TiO_2, also could produce electrons for the photocatalytic process. Furthermore, the photogenerated e- was conducive to transfer from the conduction band of TiO2 to

the interface due to the band gap of TiO2, (3.2 eV) and the lowest unoccupied molecular orbital energy level of CDs (4.2–4.4 eV) (Chen et al., 2017).

Ozone, as a selective oxidant (E=2.07 V), has been extensively applied in wastewater treatment. It is capable for decomposing various recalcitrant organic pollutants by direct ozonation and indirect use of hydroxyl radicals (•OH, E=2.8 V). Several studies reported that modifications of ozonation process, such as UV/O_3, H_2O_2/O_3 and peroxymonosulfate/O_3, was for the purpose of increasing the oxidizing capability and decomposition effectiveness of single ozonation (Pocostales et al., 2010; Yang et al., 2015; Lee et al., 2017). However, these processes required the application of high-energy UV irradiation or consumptions of large amount of oxidative chemicals. In order to improve the oxidizing ability of ozone and expanse the light adsorption wavelength, in this work, the photocatalysts TiO_2 doped with CDs, was combined with ozone as a heterogeneous photocatalysis ozonation process. Accounted for the high efficiency removal of organic pollutants and the prevention of secondary pollution, heterogeneous photocatalysis ozonation process has been reported as a promising approach of the removal of recalcitrant organic pollutants (Ikhlaq et al., 2015; Orge et al., 2015a), but investigations on modified photocatalysts combining ozone were few. As a modified ozonation process, heterogeneous photocatalysis ozonation might have significant efficiency on drinking water and wastewater treatment industries according to the formation of numerous reactive species in the process and its minimal detrimental effect on water quality (Rey et al., 2014; Quiñones et al., 2015). The superiority of the integrate process was giving rise

to the highest yield of reactive species such as •OH, $O_2^{\bullet -}$, h^+, etc. Additionally, heterogeneous photocatalytic ozonation process belongs to a complicated gas-liquid-solid process which contains numerous reactive species, electron transfer, surface reaction steps and catalytic photoexcitation process. Hence, massive redox reactions involved different steps and schematic photocatalytic ozonation mechanism were proposed in this study.

Among the advanced oxidation processes (AOPs), the combination of photocatalytic oxidation and ozonation process could lead to higher mineralization and degradation rate of PPCPs compare with the effect achieved by single process. As a matter of fact, a synergistic effect has been reported between photocatalysts and ozone due to the powerful electron trapping ability of ozone, the recombination of electron-hole pairs was suppress to some extend and resulted in the formation of ozonide ion radical $O_3^{\bullet -}$, which eventually transform into •OH (Černigoj et al., 2007).

As photocatalytic activity evaluation of TiO_2/CDs under simulated sunlight irradiation has been previously investigated in our work. For the practical application of photocatalytic process, the joint use of ozone with photocatalysts would be an advantage. In this study, TiO_2/CDs and ozone was conducted under simulated sunlight irradiation with the purpose of decomposing CIP. Due to the generation of hydroxyl radicals (•OH), superoxide ion radical ($O_2^{\bullet -}$) and other reactive species, heterogeneous photocatalysis ozonation process has been demonstrated to be efficient in organic pollutant decomposition.

2. Experimental

2.1 Material

Ciprofloxacin (CIP, 98%) and commercial TiO_2 were purchased from TCI Reagent Co. Ltd. (China). 4-chloro-7-nitrobenzo-2-oxa-1,3-diazole (NBD-Cl), tert-Butyl alcohol and benzoquinone were purchased from Aladdin (China). HPLC-grade acetonitrile and methanol were obtained from CNW Technologies GmbH (Germany). Analytical grade citric acid, urea, $Na_2C_2O_4$, potassium dichromate and sodium azide were obtained from Taitan (China). Ozone was introduced by an ozone generator (Quanju Technology, China) fed with pure oxygen (99.5%). Ultrapure water (18.25 $M\Omega \cdot cm^{-1}$) collected from Milli-Q apparatus (Germany) was used in the preparation of all aqueous solutions during the experiment. All chemical reagents were used as received without further purification. Secondary wastewater effluent was collected from Guangzhou wastewater treatment plant (WWTP) and Pearl River water was collected from Zhujiang (Guangzhou).

2.2 Preparation of photocatalysts

2.2.1 Preparation of NCDs

Carbon dots (CDs) were synthesized by hydrothermal method (Qu et al., 2012). In this study, 3.0g urea and 3.0g citric acid were added with 10mL ultrapure water in a beaker. The mixture was stirred for 10 min and then transferred into a 100 mL Teflon autoclave at 180 ◦C for 5 h. After cooling down to room temperature, the collected solution would be centrifuged at 10000 rpm for 30 min to get rid of large particles.

The remaining CDs solution was placed at 70 ◦C to receive desiccated CDs powders. At last, the powders were suspended in ultrapure water to receive 20g·L^{-1} stock solution.

2.2.2 Preparation of TiO_2/CDs photocatalysts

In this study, the TiO_2/CDs were synthesized by a facile hydrothermal-calcination method. A weighed quality (0.5g) of TiO_2 was dispersed in 30mL ethanol in an alumina crucible with continuous magnetic stirring. Afterwards, the calculated quality of CDs (TiO_2/CDs molar ratio of 0, 2.0%, 4.0%, 6.0%, 8.0%) were added into the TiO_2 suspension and vaporized at 75 ◦C. Then, the substance was heated in a muffle furnace at 300 ◦C for 3h with a heating rate of 5 ◦C·min^{-1}. Finally, the obtained products were labeled as TiO_2, 2.0 wt%, 4.0 wt%, 6.0 wt% and 8.0 wt% of TiO_2/CDs, respectively.

2.3. Characterization methods

The crystallinity of the obtained samples was characterized by X-ray diffraction (XRD Bruker-D8-Advanced X-ray diffractometer) with Cu Kα radiation and scan area of 2θ from 10° to 80°. The microscopic morphology of the samples were observed by a transmission electron microscope (TEM, JEM-2100HR) and scanning electron microscope (SEM, JSM-6700). X-ray photoelectron spectroscopy (XPS) was applied to analyze the chemical components and ionic characteristics, which equipped a Thermo VG ESCALAB 250 spectrometer with Al Kα radiation as excitation source.

The Fourier transform infrared (FT-IR) spectra were recorded by a Nicolet 6700 spectrophotometer (Thermofisher) in the range from 4000 to 400 cm^{-1}.

2.4 Photocatalysis, ozonation and photocatalytic ozonation experiments

The efficiency of photocatalytic ozonation were evaluated by the degradation of CIP. The experiment was conducted in a XPA-7 rotary photochemical reactor with ozone bubbled at the bottom of the reactor with flow rate of 15 $mL \cdot min^{-1}$ (Nanjing Xujiang machine plant). 350 W xenon lamp with 290 nm cut-off filters were utilized to simulate sunlight source. In a typical process, 50 mg photocatalysts were introduced into 50 mL of CIP aqueous solution in a 50 mL quartz tube. Before illumination, the solution was magnetic stirred in the dark for 30 min to ensure the adsorption/desorption equilibrium for CIP on the photocatalysts. When the xenon lamp was connected, the ozone bubbled at the bottom of the reactor simultaneously. At given time intervals, 2.0 mL samples were withdrawn and mixed with 0.5 mL $Na_2S_2O_3$ solution to quench residual O_3. Prior to HPLC analysis, the samples were filtered with 0.22 μm Millipore filters to remove particles. Additionally, single photocatalysis, single ozonation, and photolysis were also conducted under identical condition.

2.5 . Analytical methods

The concentration of CIP was determined by high performance liquid chromatography (HPLC, waters e2695). The concentration of ozone in aqueous

199 solution was determined by the indigo method (Bader and Hoigné, 2013). 200
200 μmol·L^{-1} NBD-Cl was applied as the fluorescent probe to determine the amount of
201 $O_2^{\bullet-}$ (Olojo et al., 2005; Ikhlaq et al., 2013). The degradation intermediates yielded
202 during the photocatalytic ozonation process was identified by the application of
203 high-resolution accurate-mass spectrometry (HRAM) LC-MS/MS, which included a
204 Q Exactive Orbitrap mass spectrometer and HPLC system (Ultimate 3000RSLC,
205 Thermo Scientific, USA). The intermediates was separated by the employment of a
206 Hypersil GOLD C18 (100 x 2.1 mm, 1.9 μm).

207 Linearity of the analysis was constructed with calibration range of 0.02-5.00 μg/ml
208 (0.02, 0.05, 0.10, 0.50, 2.00, 5.00 μg/ml) for HPLC analysis. The regression
209 coefficients were ≥0.99 for liner calibration curves. The limits of detection (LOD) and
210 quantification (LOQ) for CIP was 3.3 ng/ml and 11 ng/ml, which was calculated as
211 signal-to-noise ratio (S/N)=3:1 and 10:1, respectively.

212

213 **3. Results and discussion**

214 The XRD pattern of pure TiO_2 and different contents of CDs on TiO_2 were
215 displayed in Fig. S1. The diffraction peaks of the photocatalysts were sharp,
216 indicating high degree crystallinity was in the sample structures. As observed from
217 XRD patterns, the rutile form TiO_2 (represented by R) had reflections at 2θ=25.3°,
218 37.9°, 48.0°, 54.2° and 55.2°, which corresponding to (101), (004), (200), (105), (211),
219 (204) and (220). The result is consistent with anatase crystal phase for TiO_2 (JCPDS
220 PDF#: 00-021-1272). Implying that the CDs doping did not significantly alter the

crystal structure of TiO_2.

In order to confirm the morphologies of the photocatalysts, pristine TiO_2 and 6 wt% TiO_2/CDs were characterized by SEM. As depicted in Fig. S2 (a-c), providing visualization of the structural characteristics of the materials, indicated that the material had a globular shape (Lu et al., 2018). Additionally, the textural characterization of pristine was practically the same as the 6 wt% TiO_2/CDs. As confirmed in the TEM images of 6 wt% TiO_2/CDs (Fig. S2 d-e), the CDs were well loaded on the surface of the photocatalysts. The clear lattice fringes of TiO_2 (d = 0.35 nm) showed uniformity corresponding to (101) crystal plane of anatase TiO_2. (Sajjad et al., 2009) The selected area electron diffraction (SAED) pattern of 6 wt% TiO_2/CDs showed that the photocatalysts was polycrystalline in nature.

The surface chemical compositions of prepared 6 wt% TiO2/CDs was determined by XPS. As depicted in Fig. S3(a), the survey spectrum detected the presence of titanium (Ti 2p), carbon (C 1s), and oxygen (O 1s) in 6 wt% TiO2/C-Dots, which suggested that the prepared material was mainly composed of Ti, C and O elements. In Fig. S3(b), two peaks at 458.2 and 464.1 eV in the Ti 2p spectrum corresponded to the the $Ti2p_{3/2}$ and Ti $2p_{1/2}$, respectively (Khan et al., 2018). In Fig. 3(c), three peaks at 284.3, 286.1 and 287.9 eV were observed in high-resolution XPS spectrum of C 1s. Respectively, the peak at 284.3 eV was attributed to C-C groups; the peak at 286.1 eV was attributed to C-O groups and the peak 287.9 eV was attributed to C=O groups (Yu and Kwak, 2012). Three peaks were noticed as the O 1s XPS spectrum showed in Fig. 3(d), the peak at 529.7 eV was assigned to Ti–O; the peak at 530.5 eV was assigned to

the surface –OH groups and the peak at 532.2 eV was assigned to C=O groups (Liu et al., 2011; Li et al., 2018). The above results demonstrated the well establishment of CDs doping on TiO_2.

3.1 Degradation of CIP

3.1.1 photocatalytic activity

The efficiency of as-prepare sunlight-driven TiO_2/CDs collaborate with ozonation was evaluated by the degradation of CIP. Pyrex glasses were conducted as wavelength filters for UVC waveband (200–275 nm) and a part of the UVB waveband (275–290 nm) in the experiment. As Fig. 1(a) displayed, the concentration of CIP barely changed under single photocatalysis, indicating that CIP was stable to simulated sunlight irradiation. Similar phenomenon was reported by Wang et al (Wang et al., 2017a). After the introduction of TiO_2, slight degradation of CIP was observed. Observed from the result, the degradation rate was enhanced after CDs doped on TiO_2. For comparison, 64% of CIP was decomposed by pristine TiO_2 in 30 min while 91.1% of degradation rate was achieved by minor introduction of CDs (1.0 wt%). Suggesting the ratio of TiO_2/CDs significantly correlated with the catalytic activity as mentioned in previous section. An optimum result was achieved by 6 wt% CDs contents on the TiO_2, which was determined to be the optimal concentration of CDs content on TiO_2, further increasing would result in a decrease in the photocatalytic activity for CIP degradation.

Fig. 1

3.1.2 photocatalytic ozonation experiment

By means of generating hydroxyl radicals (Table S1), solo ozonation itself could decompose a part of CIP in the given time. But, still, it was not efficient and complete. Additionally, the joint use of photocatalysts and ozone exhibited strong degradation efficiency of CIP. As Fig. 1(b) showed, the degradation rate of photocatalytic ozonation fitted pseudo-first-order kinetic model well. Compare with ozone alone (k=0.083), the combination of photocatalysts and ozone achieved much higher degradation rates. Notably, when photocatalysis and ozonation were carried out simultaneously, 99.7% CIP was decomposed in 16 min by 6 wt% TiO_2/CDs and ozone, which was much higher than the sum of the single performance of 6 wt% TiO_2/CDs and ozone. Additionally, among the above mentioned process, 6 wt% TiO_2/CDs remained the optimal achievement and brought the highest degradation rate of CIP. For comparison, the optimal degradation rate constant was 0.32, which was about 2.48 times of 6 wt% TiO_2/CDs without ozone (k=0.129).

3.1.3 Influence of different initial pH value

The investigation of pH value is necessary for photocatalytic ozonation as it has effects on the utilization efficiency of ozone and properties of photocatalysts surface. As mentioned by Levanov et al.(Levanov et al., 2018), at higher pH, hydroxide (OH^-)

287 could initiate a chain reaction of ozone decomposition and result in higher amount of
288 •OH. Hence, in single ozone process, higher degradation efficiency would achieve at
289 alkaline pH. As shown in Fig. 1(c), alkaline pH lead to the higher degradation
290 efficiency in photocatalytic ozonation process. However, instead of continuously
291 increasing, the efficiency increment was retarded in higher pH. Since the pKa of CIP
292 has been reported to be 6.16 and 8.23, also could be negatively and positively charged
293 under various pH value which was depicted in Fig. S4 (Giri and Golder, 2014). Which
294 means CIP present in cationic form at pH＜6.16, in zwitterionic form at pH 6.16-8.23
295 and in anionic form at pH＞8.23. During photocatalytic ozonation process, the surface
296 properties of the photocatalysts could be affected by different pH, resulting from the
297 proton transference (Chen et al., 2014). The isoelectric point of 6 wt% TiO_2/CDs was
298 approximately 3.3 according to zeta potential report in Fig. S5, indicating the surface
299 of the photocatalysts has negative charge at pH＞3.3. In this case, repulsive force
300 occurred between CIP and the photocatalysts while pH＞8.23 and further intensified
301 as pH increased, resulted in a lower CIP degradation efficiency. Which reached a
302 balance with continuously generated •OH and explained the phenomenon.
303
304 3.2 Reactive species and mechanism
305 Previous studies have indicated that multiple reactive species (RSs), like •OH,
306 $O_2^{\bullet-}$, h^+, $^1O_2$ and e^- would generated during the photocatalytic ozonation process
307 (Nawrocki and Kasprzyk-Hordern, 2010). In order to quantitatively determine the role
308 of reactive species, quenching experiment was conducted by tert-Butyl alcohol (TBA

309 10mM), benzoquinone (BQ 1.0mM), $Na_2C_2O_4$ 10mM, potassium dichromate (K_2CrO_4
310 50μM) and sodium azide (NaN_3 75mM). As shown in Table S1, under the control
311 experiment, a photocatalytic ozonation degradation rate constant of 0.326 min^{-1} was
312 observed. The introduction of TBA and NaN_3 significantly inhibited the degradation
313 of CIP, leading a degradation rate constant of 0.145 and 0.103 min^{-1} with a high
314 inhibition rate of 55.4% and 68.5%. From which we could deduce that the inhibition
315 rate of $^1O_2$ was 13.1%, indicating $^1O_2$ had a minor effect in the system. It could be
316 concluded that the decrement of degradation rate constant was attributed to the
317 trapping of •OH, suggesting •OH could be one of the predominant reactive species of
318 the photocatalytic ozonation process. Furthermore, the presence of BQ, $Na_2C_2O_4$ and
319 K_2CrO_4 as $O_2^{\bullet-}$, h^+ and e^- scavengers, resulting in a degradation rate constant of
320 0.237, 0.211 and 0.224 min^{-1}, with inhibition rates of 27.2%, 35.2% and 31.3%,
321 respectively. Implying that $O_2^{\bullet-}$, h^+ e^- shared an unneglectable effect in the system.

322 NBD-Cl was applied as a fluorescent probe to determine the amount of $O_2^{\bullet-}$ in
323 this study. Several researches reported the intensity of PL in the NBD-Cl products
324 would be detected at 550 nm (excited at 332 nm) if $O_2^{\bullet-}$ presence in the system and
325 interacted with NBD-Cl (Olojo et al., 2005; Ikhlaq et al., 2013). As shown in Fig. S6,
326 three samples were withdrawn under 10 min treatment of photocatalytic ozonation,
327 sole ozonation and single photocatalysts process, respectively. Fluorescent spectra
328 showed that photocatalytic ozonation process achieved the greatest amount of $O_2^{\bullet-}$
329 production. Indicating the well cooperation between the photocatalysts 6 wt%
330 TiO2/CDs and ozone.

A heterogeneous photocatalytic ozonation process involves chemical, catalytic adsorption and catalytic photoexcitation. The primary reason of CIP decomposition was the continuous generation of reactive species. In this study, the existence of ozone would have two major routes to complete the degradation of CIP in the photocatalytic ozonation process, which includes: (I) direct and indirect ozonation in the bulk. (II) Interactions on the surface of photocatalysts.

The redox potential of ozone in water is 2.07 eV, which means CIP could be decomposed by ozone directly in aqueous solution. The relevant equation and corresponding kinetic constant was exhibited in Table 1, which were proposed according to the previous scientific literatures. As shown in Eqs. 1-3, pharmaceutical could be removed by both direct and indirect mechanism where the generation of hydroxyl radicals by ozone decomposition (Mena et al., 2017). Furthermore, as illustrated in Eqs. 4-11, on the account of the breaking of aromatic rings and double carbon bond, hydrogen peroxide was generated, which was not only produced by the decomposition of ozone, but also the recombination of $\bullet O_2H$ radicals (Lovato et al., 2009; Fathinia et al., 2016). As a consequence, the hydrogen peroxide was subjected to electrons and brought in more hydroxyl radicals (Eqs. 12) (Wang et al., 2018). In sum, ozonation had the ability to transfer organic pollutants into recalcitrant intermediates.

Table 1

Under simulated sunlight irradiation, TiO_2/CDs was excited and leaded to the generation of electron-hole pair (Eqs. 13). Eqs. 14-15 showed adsorbed water molecular was oxidized by photoexcited h^+ which gave rise to the generation of •OH. Due to the lowest unoccupied molecular orbital energy level of C-Dots (4.2-4.4 eV) (Li et al., 2013) and its ability of electron migration, a mass of electron accumulation occurred on the surface of the photocatalysis. When ozone was bubbled into the photocatalytic system in the meantime, it could be adsorbed on the surface of the photocatalysis where the interactions mainly taken place (Orge et al., 2015b). As presented in Eqs. 16-17, photoexcited electron was transferred from photocatalysis surface to ozone and oxygen, therefore $O_3^{\bullet-}$ and $O_2^{\bullet-}$ were yielded, which also indicated ozone exhibit strong electrophilic property. In our previous work, during the photocatalytic process (Chen et al., 2017), both e^- and $O_2^{\bullet-}$ played negligible roles for the organic pollutants decomposition. After the introduction of ozone, electron was able to interact with oxygen molecular and lead to yield $O_2^{\bullet-}$ (Eqs. 17). According to the mechanism illustrated in Eqs. 16-20, a synergetic effect between TiO_2/CDs and ozone under simulated sunlight irradiation was proposed. Due to the electron transferred by electrophilic ozone, the reduction of electron on TiO_2/CDs resulted in the separation of electron-hole pair more effective and leaded to the continuous generation of h^+ under simulated sunlight irradiation. The photocatalytic ozonation produced reactive species could eventually lead to the completely removal of organic pollutant (Eqs. 21-23). In conclusion, the joint use of photocatalysis and ozonation possess could bring much higher •OH yield than the sum of the individual

process, which accounted for the synergistic effect between ozone and catalysts continuously separated the electrons and holes.

Table 2.

Based on above results and discussion, the probable mechanism for the photocatalytic ozonation of CIP was proposed schematically in Fig. 2. Under sunlight irradiation, the light wavelength ＞550 nm would be converted into higher-energy light (wavelength from 325 to 425 nm) on the account of the up-converted photoluminescence (PL) properties of CDs, which was adsorbed by TiO_2 and result in the generation of electron-hole pair subsequently. Moreover, the photoexcited electrons in the TiO_2 would be transferred and retained in CDs. Consequently, the electrons on the surface of CDs may interact with ozone and oxygen, leading to the generation of $O_3^{\bullet-}$ and $O_2^{\bullet-}$, which react with other reactive species to generate •OH. Eventually, the presence of reactive species $O_2^{\bullet-}$, h^+, •OH and O_3 would lead to the decomposition of CIP.

The presence of CDs obviously enhances the removal efficiency of CIP, which attributes to its multiple functions when doped on the TiO_2. In conclusion, there mainly involves three major functions of CDs in this study: (1) Light adsorption efficiency enhancement (2) Extraordinary electron transfer ability (3) High-capacity of electron storage.

Fig.2

3.3 Transformation pathways of CIP

HRAM LC-MS/MS was applied to identify the intermediates yielded by the photocatalytic ozonation of CIP and the possible molecular structure of the intermediates were proposed according to the analysis of mass spectrum (Fig. S7). The molecular masses, retention time and structures of twelve identified intermediates were summarized in Table S2. The transformation pathway of CIP during photocatalytic ozonation process was deduced schematically in the Fig. 3.

In the pathway I, N (4) in the piperazine ring were attack by •OH and lead to the H atom on N (4) replaced by hydrogen bond, which indicated compound P1 (348.13417) should be ascribed as piperazine oxidation. Subsequently, P5 (362.11412) was formed after the hydroxyl bond was further oxidized into two aldehyde groups on N (1) and N (4). The cleavage of each C═O bond on N (1) and N (4) resulted in the formation of P8 (334.11957) and P9 (334.12041). Meanwhile, P10 (344.10410) was originated from the defluorination of P5 (362.11412) The continuous oxidation on bond cleavage leaded to the molecular weight of intermediate products decreased, the formation of P12 (263.08253) and P13 (245.11444) demonstrated CIP had been effectively decomposed in the photocatalytic ozonation process.

In the pathway II, P2 (348.13506) resulted from the electrophilic adduct reaction arose on C (15), leading to the addition of hydroxyl radical to the parent molecule. Further, P6 (288.07837) was formed after P2 (348.13506) underwent quinolonic ring

419 oxidation, resulting in the cleavage of hydroxyl bond and decarboxylation (Diao et al.,
420 2016).

421 In the pathway III, the reaction was initiated by the attack on F (16), which
422 underwent a hydroxyl radical substitution, resulting in the formation of P3 (330.12482)
423 defluorination product. According to our previous work, based on the calculated
424 frontier electron densities (FEDs) of CIP, compound P5 (362.11412) in pathway I was
425 attack by $O_2^{\bullet-}$ and $^1O_2$, meanwhile pathway III was initiated by $O_2^{\bullet-}$ and •OH. As
426 FEDs of CIP was calculated to predict the reaction sites (An et al., 2010), which
427 directly demonstrated the presence of $O_2^{\bullet-}$, •OH, and $^1O_2$ in this study.

428 Pathway IV belongs to the degradation at the quinolone moiety. The cleavage of C
429 (14) and C (15) carbon–carbon double bond adjacent to the carboxylic acid group
430 gave rise to the formation of ketone product P4 (336.12424). The fractured quinolonic
431 ring closed up afterwards with the loss of carboxyl, leading to the formation of
432 diketone P7 (290.26767). Then the N (1) and N (4) atoms underwent the attack by
433 RSs, resulted in the loss of $-C_2H_2$ on the piperazine ring and gave rise to P11
434 (264.08218). Similar reaction pathway was occurred by Dewitte et al (Dewitte et al.,
435 2008), which was triggered by ozone from his perspective. Eventually, CIP and its
436 oxidized intermediates would be completely decomposed to inorganic matters such as
437 CO_2, NO_3^-, F^-, H_2O in the following prolonged time.

438

439 Fig. 3

440

441 3.4 Effects of water constituents and matrices

442 In order to investigate the photocatalytic ozonation performance in practical
443 application, influence of commonly existed inorganic anions, cations and humic acid
444 (HA) were carried out in this study. The impact of inorganic anions (including NO_3^-,
445 NO_2^-, CO_3^{2-}, HCO_3^-, Cl^-, SO_4^{2-}) were carried out at fixed concentration of 5 mM.
446 As depicted in Fig. 4(a), except the negligible effect of SO_4^{2-}, all inorganic anions
447 showed various inhibitory influences on the CIP degradation. The k_{obs} of the control
448 experiment was 0.32 min^{-1} ,while the addition of NO_3^-,NO_2^-,CO_3^{2-},HCO_3^-,Cl^-,SO_4^{2-}
449 leaded to the reduced k_{obs} of 0.23, 0.05, 0.12, 0.2, 0.29 and 0.31 min^{-1}, respectively.
450 Nitrite (NO_2^-), especially, showed a great inhibitory effect on the photocatalytic
451 process. In aqueous solution, NO_2^- could be oxidized into NO_3^- by powerful
452 oxidant such as ozone and •OH (Schroeder et al., 2011). Afterwards, as an electron
453 trapper and competing with ozone (NavíO et al., 1998), NO_3^- showed inhibitory
454 effect as well. Same phenomenon occurred by Yang et al (Yang et al., 2018). As
455 commonly detected ions in industrial wastewater, NO_3^- and NO_2^- might show
456 disadvantages for photocatalytic ozonation process. The presence of HA, CO_3^{2-} and
457 HCO_3^- also showed inhibitory effect on the CIP degradation, which might be
458 ascribed to their high efficiency of reactive species scavenging (Feng et al., 2017).
459 Additionally, HA could adsorb a part of sunlight in aqueous solution and resulted in
460 the detrimental effect of photocatalytic performance. (Zhou et al., 2013) On the other
461 hand, no obvious effect on the removal of CIP was found in the presence of Cl^-, SO_4^{2-}
462 . Furthermore, the divalent metal cations, Ca^{2+} and Mg^{2+} led to the decline of CIP

463 degradation which may attribute to the scavenging of electrons (And and Madras,
464 2007).

465 In order to evaluate the feasibility of the photocatalytic ozonation process under
466 ambient condition, WWTP water and Pearl River were carried out as solvent of CIP to
467 compare with ultrapure water. As depicted in Fig. 4(b), though slight inhibitory effects
468 were shown, the photocatalytic ozonation process still exhibit well performance in
469 wastewater. The inhibitory effect might attribute to the high TOC value in wastewater,
470 which would consume the reactive species in the process. In addition, high turbidity
471 of the wastewater also could affect the degradation efficiency by weakening light
472 absorption(Wang et al., 2018). In conclusion, photocatalytic ozonation process of
473 TiO_2/CDs under simulated sunlight irradiation could show high efficiency in
474 wastewater treatment.

475 Fig. 4

476

477 **4. Conclusion**

478 In this work, we construct a high-efficiency heterogeneous system by 6 wt%
479 TiO_2/CDs and ozone under simulated sunlight irradiation. The performance of
480 photocatalytic ozonation process was superior to photocatalysis and single ozonation.
481 Owing to the higher separation efficiency of photogenerated electron-holes and the
482 richer generation of reactive species, fast removal of CIP was achieved. Mechanism
483 studies revealed that the present of CDs played a significant role in this process.
484 Besides the up-converted PL properties of CDs, the ability of electron accumulation

485 accelerating the process of electron transferred on ozone and oxygen was not
486 neglectable. Moreover, the pH investigation deduced that a balance took place
487 between the repulsive force and larger amount of •OH, resulted in limits of
488 degradation rate constant in further increasing pH. This work is favorable for the
489 understanding in photocatalytic ozonation reaction mechanism, as well as the
490 transformation of CIP during the process and the effects of natural water constituents
491 on the kinetics.

492

493 **Acknowledgements**

494 This work was supported by the National Natural Science Foundation of China
495 No.21377031 and 21677040), Science and Technology Planning Project of
496 Guangdong Province (No. 2017A050506052).

497

498

499 **References**

500 An, T., Yang, H., Li, G., Song, W., Cooper, W.J., Nie, X., 2010. Kinetics and mechanism of advanced
501 oxidation processes (AOPs) in degradation of ciprofloxacin in water. Applied Catalysis B: Environmental
502 94, 288-294.
503 And, T.A., Madras, G., 2007. Photocatalytic Degradation of Rhodamine Dyes with Nano-TiO2. Industrial
504 & Engineering Chemistry Research 46, 1-7.
505 Bader, H., Hoigné, J., 2013. Determination of ozone in water by the indigo method. Water Research 15,
506 449-456.
507 Černigoj, U., Štangar, U.L., Trebše, P., 2007. Degradation of neonicotinoid insecticides by different
508 advanced oxidation processes and studying the effect of ozone on TiO2 photocatalysis. Applied
509 Catalysis B: Environmental 75, 229-238.
510 Chen, J., Wen, W., Kong, L., Tian, S., Ding, F., Xiong, Y., 2014. Magnetically Separable and Durable
511 MnFe2O4 for Efficient Catalytic Ozonation of Organic Pollutants. Industrial & Engineering Chemistry
512 Research 53, 6297–6306.
513 Chen, P., Wang, F., Chen, Z.F., Zhang, Q., Su, Y., Shen, L., Yao, K., Liu, Y., Cai, Z., Lv, W., 2017. Study on
514 the photocatalytic mechanism and detoxicity of gemfibrozil by a sunlight-driven TiO 2 /carbon dots
515 photocatalyst: The significant roles of reactive oxygen species. Applied Catalysis B Environmental 204,

250-259.
Dewitte, B., Dewulf, J., Demeestere, K., Van, D.V.V., De, W.P., Van, L.H., 2008. Ozonation of ciprofloxacin in water: HRMS identification of reaction products and pathways. Environmental Science & Technology 42, 4889-4895.
Diao, Z.H., Xu, X.R., Jiang, D., Li, G., Liu, J.J., Kong, L.J., Zuo, L.Z., 2016. Enhanced catalytic degradation of ciprofloxacin with FeS2/SiO2 microspheres as heterogeneous Fenton catalyst: Kinetics, reaction pathways and mechanism. Journal of Hazardous Materials 327, 108.
Doorslaer, X.V., Dewulf, J., Langenhove, H.V., Demeestere, K., 2014. Fluoroquinolone antibiotics: An emerging class of environmental micropollutants. Science of the Total Environment 500-501, 250-269.
Erik, G., Sha, C., Berg, O.G., Carolina, I.C., Linus, S., Diarmaid, H., Dan, I., Andersson, 2011. Selection of resistant bacteria at very low antibiotic concentrations. Plos Pathogens 7, e1002158.
Fang, S., Xia, Y., Lv, K., Li, Q., Sun, J., Li, M., 2016. Effect of carbon-dots modification on the structure and photocatalytic activity of g-C3N4. Applied Catalysis B: Environmental 185, 225-232.
Fathinia, M., Khataee, A., Aber, S., Naseri, A., 2016. Development of kinetic models for photocatalytic ozonation of phenazopyridine on TiO2 nanoparticles thin film in a mixed semi-batch photoreactor. Applied Catalysis B: Environmental 184, 270-284.
Feng, Y., Song, Q., Lv, W., Liu, G., 2017. Degradation of ketoprofen by sulfate radical-based advanced oxidation processes: Kinetics, mechanisms, and effects of natural water matrices. Chemosphere 189, 643-651.
Giri, A., Golder, A., 2014. Ciprofloxacin degradation from aqueous solution by Fenton oxidation: reaction kinetics and degradation mechanisms. Rsc Advances 4, 6738-6745.
Ikhlaq, A., Brown, D.R., Kasprzyk-Hordern, B., 2013. Mechanisms of catalytic ozonation: An investigation into superoxide ion radical and hydrogen peroxide formation during catalytic ozonation on alumina and zeolites in water. Applied Catalysis B Environmental 129, 437-449.
Ikhlaq, A., Brown, D.R., Kasprzyk-Hordern, B., 2015. Catalytic ozonation for the removal of organic contaminants in water on alumina. Applied Catalysis B: Environmental 165, 408-418.
Kenny, O., Marion-Justine, C., Thierry, B., Hélène, B., Fabienne, P., 2012. Evidence for a complex relationship between antibiotics and antibiotic-resistant Escherichia coli: from medical center patients to a receiving environment. Environmental Science & Technology 46, 1859.
Khan, H., Rigamonti, M.G., Patience, G.S., Boffito, D.C., 2018. Spray dried TiO2/WO3 heterostructure for photocatalytic applications with residual activity in the dark. Applied Catalysis B: Environmental 226, 311-323.
Kümmerer, K., 2009. Antibiotics in the aquatic environment – A review – Part I. Chemosphere 75, 417-434.
Lee, M., Merle, T., Rentsch, D., Canonica, S., von Gunten, U., 2017. Abatement of Polychoro-1,3-butadienes in Aqueous Solution by Ozone, UV Photolysis, and Advanced Oxidation Processes (O3/H2O2 and UV/H2O2). Environmental Science & Technology 51, 497-505.
Levanov, A.V., Isaikina, O.Y., Gasanova, R.B., Lunin, V.V., 2018. Solubility of Ozone and Kinetics of Its Decomposition in Aqueous Chloride Solutions. Industrial & Engineering Chemistry Research 57, 14355-14364.
Li, R., Cai, M., Xie, Z., Zhang, Q., Zeng, Y., Liu, H., Liu, G., Lv, W., 2019. Construction of heterostructured CuFe2O4/g-C3N4 nanocomposite as an efficient visible light photocatalyst with peroxydisulfate for the organic oxidation. Applied Catalysis B: Environmental 244, 974-982.
Li, Y., Liu, Z., Wu, Y., Chen, J., Zhao, J., Jin, F., Na, P., 2018. Carbon dots-TiO 2 nanosheets composites for

photoreduction of Cr(VI) under sunlight illumination: favorable role of carbon dots. Applied Catalysis B Environmental 224.

Li, Y., Zhang, B.P., Zhao, J.X., Ge, Z.H., Zhao, X.K., Zou, L., 2013. ZnO/carbon quantum dots heterostructure with enhanced photocatalytic properties, Appl. Surf. Sci (In press). Applied Surface Science 279, 367-373.

Liu, J.W., Han, R., Wang, H.T., Zhao, Y., Lu, W.J., Wu, H.Y., Yu, T.F., Zhang, Y.X., 2011. Degradation of PCP-Na with La–B co-doped TiO 2 series synthesized by the sol–gel hydrothermal method under visible and solar light irradiation. Journal of Molecular Catalysis A Chemical 344, 145-152.

Lovato, M.E., Martín, C.A., Cassano, A.E., 2009. A reaction kinetic model for ozone decomposition in aqueous media valid for neutral and acidic pH. Chemical Engineering Journal 146, 486-497.

Lu, Y., Zhang, X., Chu, Y., Yu, H., Huo, M., Qu, J., Crittenden, J.C., Huo, H., Yuan, X., 2018. Cu2O nanocrystals/TiO2 microspheres film on a rotating disk containing long-afterglow phosphor for enhanced round-the-clock photocatalysis. Applied Catalysis B: Environmental 224, 239-248.

Martins, N.C.T., Ângelo, J., Girão, A.V., Trindade, T., Andrade, L., Mendes, A., 2016. N-doped carbon quantum dots/TiO2 composite with improved photocatalytic activity. Applied Catalysis B: Environmental 193, 67-74.

Mena, E., Rey, A., Rodríguez, E.M., Beltrán, F.J., 2017. Reaction mechanism and kinetics of DEET visible light assisted photocatalytic ozonation with WO3 catalyst. Applied Catalysis B: Environmental 202, 460-472.

NavíO, J.A., Colón, G., Trillas, M.A., Peral, J., Domènech, X., Testa, J.J., Padrón, J., RodríGuez, D., Litter, M.I., 1998. Heterogeneous photocatalytic reactions of nitrite oxidation and Cr(VI) reduction on iron-doped titania prepared by the wet impregnation method. Applied Catalysis B Environmental 16, 187-196.

Nawrocki, J., Kasprzyk-Hordern, B., 2010. The efficiency and mechanisms of catalytic ozonation. Applied Catalysis B: Environmental 99, 27-42.

Olojo, R.O., Xia, R.H., Abramson, J.J., 2005. Spectrophotometric and fluorometric assay of superoxide ion using 4-chloro-7-nitrobenzo-2-oxa-1,3-diazole. Analytical Biochemistry 339, 338-344.

Orge, C.A., Pereira, M.F.R., Faria, J.L., 2015a. Photocatalytic ozonation of model aqueous solutions of oxalic and oxamic acids. Applied Catalysis B: Environmental 174-175, 113-119.

Orge, C.A., Pereira, M.F.R., Faria, J.L., 2015b. Photocatalytic ozonation of model aqueous solutions of oxalic and oxamic acids. Applied Catalysis B Environmental 174-175, 113-119.

Pocostales, J.P., Sein, M.M., Knolle, W., von Sonntag, C., Schmidt, T.C., 2010. Degradation of Ozone-Refractory Organic Phosphates in Wastewater by Ozone and Ozone/Hydrogen Peroxide (Peroxone): The Role of Ozone Consumption by Dissolved Organic Matter. Environmental Science & Technology 44, 8248-8253.

Qu, S., Wang, X., Lu, Q., Liu, X., Wang, L., 2012. A Biocompatible Fluorescent Ink Based on Water‐Soluble Luminescent Carbon Nanodots. Angewandte Chemie 124, 12381-12384.

Quiñones, D.H., Rey, A., Álvarez, P.M., Beltrán, F.J., Puma, G.L., 2015. Boron doped TiO 2 catalysts for photocatalytic ozonation of aqueous mixtures of common pesticides: Diuron, o-phenylphenol, MCPA and terbuthylazine. Applied Catalysis B Environmental 178, 74-81.

Rey, A., García-Muñoz, P., Hernández-Alonso, M.D., Mena, E., García-Rodríguez, S., Beltrán, F.J., 2014. WO 3 –TiO 2 based catalysts for the simulated solar radiation assisted photocatalytic ozonation of emerging contaminants in a municipal wastewater treatment plant effluent. Applied Catalysis B Environmental 154-155, 274-284.

Rodriguez-Mozaz, S., Chamorro, S., Marti, E., Huerta, B., Gros, M., Sànchez-Melsió, A., Borrego, C.M., Barceló, D., Balcázar, J.L., 2015. Occurrence of antibiotics and antibiotic resistance genes in hospital and urban wastewaters and their impact on the receiving river. Water Research 69, 234-242.

Sajjad, A.K.L., Shamaila, S., Tian, B., Chen, F., Zhang, J., 2009. One step activation of WOx/TiO2 nanocomposites with enhanced photocatalytic activity. Applied Catalysis B: Environmental 91, 397-405.

Schroeder, J.P., Croot, P.L., Dewitz, B.V., Waller, U., Hanel, R., 2011. Potential and limitations of ozone for the removal of ammonia, nitrite, and yellow substances in marine recirculating aquaculture systems. Aquacultural Engineering 45, 35-41.

Steenbergen, J., Tanaka, S.K., Miller, L.L., Halasohoris, S.A., Hershfield, J.R., 2017. In VitroandIn VivoActivity of Omadacycline against Two Biothreat Pathogens,Bacillus anthracisandYersinia pestis. Antimicrobial Agents & Chemotherapy 61, AAC.02434-02416.

Verlicchi, P., Al, A.M., Zambello, E., 2012. Occurrence of pharmaceutical compounds in urban wastewater: removal, mass load and environmental risk after a secondary treatment--a review. Science of the Total Environment 429, 123-155.

Wang, B., Di, J., Zhang, P., Xia, J., Dai, S., Li, H., 2017a. Ionic liquid-induced strategy for porous perovskite-like PbBiO2Br photocatalysts with enhanced photocatalytic activity and mechanism insight. Applied Catalysis B: Environmental 206, 127-135.

Wang, F., Chen, P., Feng, Y., Xie, Z., Liu, Y., Su, Y., Zhang, Q., Wang, Y., Yao, K., Lv, W., Liu, G., 2017b. Facile synthesis of N-doped carbon dots/g-C3N4 photocatalyst with enhanced visible-light photocatalytic activity for the degradation of indomethacin. Applied Catalysis B: Environmental 207, 103-113.

Wang, F., Feng, Y., Chen, P., Wang, Y., Su, Y., Zhang, Q., Zeng, Y., Xie, Z., Liu, H., Liu, Y., Lv, W., Liu, G., 2018. Photocatalytic degradation of fluoroquinolone antibiotics using ordered mesoporous g-C3N4 under simulated sunlight irradiation: Kinetics, mechanism, and antibacterial activity elimination. Applied Catalysis B: Environmental 227, 114-122.

Wang, F., Wu, Y., Wang, Y., Li, J., Jin, X., Zhang, Q., Li, R., Yan, S., Liu, H., Feng, Y., Liu, G., Lv, W., 2019. Construction of novel Z-scheme nitrogen-doped carbon dots/{0 0 1} TiO2 nanosheet photocatalysts for broad-spectrum-driven diclofenac degradation: Mechanism insight, products and effects of natural water matrices. Chemical Engineering Journal 356, 857-868.

Wen, M.Q., Xiong, T., Zang, Z.G., Wei, W., Tang, X.S., Dong, F., 2016. Synthesis of MoS2/g-C3N4 nanocomposites with enhanced visible-light photocatalytic activity for the removal of nitric oxide (NO). Optics Express 24, 10205.

Xie, Z., Feng, Y., Wang, F., Chen, D., Zhang, Q., Zeng, Y., Lv, W., Liu, G., 2018. Construction of carbon dots modified MoO3/g-C3N4 Z-scheme photocatalyst with enhanced visible-light photocatalytic activity for the degradation of tetracycline. Applied Catalysis B: Environmental 229, 96-104.

Yang, T., Peng, J., Zheng, Y., He, X., Hou, Y., Wu, L., Fu, X., Yang, T., Peng, J., Zheng, Y., 2018. Enhanced photocatalytic ozonation degradation of organic pollutants by ZnO modified TiO 2 nanocomposites. Applied Catalysis B Environmental 221.

Yang, Y., Jiang, J., Lu, X., Ma, J., Liu, Y., 2015. Production of sulfate radical and hydroxyl radical by reaction of ozone with peroxymonosulfate: a novel advanced oxidation process. Environmental Science & Technology 49, 7330-7339.

Ye, Y., Zang, Z., Zhou, T., Dong, F., Lu, S., Tang, X., Wei, W., Zhang, Y., 2018. Theoretical and experimental investigation of highly photocatalytic performance of CuInZnS nanoporous structure for

removing the NO gas. Journal of Catalysis 357, 100-107.
Yu, B.Y., Kwak, S.Y., 2012. Carbon quantum dots embedded with mesoporous hematite nanospheres as efficient visible light-active photocatalysts. Journal of Materials Chemistry 22, 8345-8353.
Zhang, Q.-Q., Ying, G.-G., Pan, C.-G., Liu, Y.-S., Zhao, J.-L., 2015. Comprehensive Evaluation of Antibiotics Emission and Fate in the River Basins of China: Source Analysis, Multimedia Modeling, and Linkage to Bacterial Resistance. Environmental Science & Technology 49, 6772-6782.
Zhang, Q., Chen, P., Tan, C., Chen, T., Zhuo, M., Xie, Z., Wang, F., Liu, H., Cai, Z., Liu, G., Lv, W., 2018a. A photocatalytic degradation strategy of PPCPs by a heptazine-based CN organic polymer (OCN) under visible light. Environmental Science: Nano 5, 2325-2336.
Zhang, Q., Chen, P., Zhuo, M., Wang, F., Su, Y., Chen, T., Yao, K., Cai, Z., Lv, W., Liu, G., 2018b. Degradation of indometacin by simulated sunlight activated CDs-loaded BiPO4 photocatalyst: Roles of oxidative species. Applied Catalysis B: Environmental 221, 129-139.
Zhou, L., Ji, Y., Zeng, C., Zhang, Y., Wang, Z., Yang, X., 2013. Aquatic photodegradation of sunscreen agent p -aminobenzoic acid in the presence of dissolved organic matter. Water Research 47, 153-162.
Zhou, Z., Jiang, J.Q., 2015. Reaction kinetics and oxidation products formation in the degradation of ciprofloxacin and ibuprofen by ferrate(VI). Chemosphere 119, S95-S100.

Table 1. Reactions and kinetic constant of ozone in bulk solution at pH 7

Reaction No.	Reaction	Kinetic constant	references
1	$O_3 + CIP \rightarrow intermediates$	—	(Mena et al., 2017)
2	$O_3 + OH^- \rightarrow HO_2^- + O_2$	70 $M^{-1}s^{-1}$	(Mena et al., 2017)
3	$O_3 + HO_2^- \rightarrow HO\cdot + O_3^{\bullet -}$	2.8×10^6 $M^{-1}s^{-1}$	(Mena et al., 2017)
4	$O_3 + OH\cdot \rightarrow HO_2\cdot + O_2$	2×10^9 $M^{-1}s^{-1}$	(Fathinia et al., 2016)
5	$O_2 + e^- \rightarrow O_2^{\bullet -}$	—	(Fathinia et al., 2016)
6	$O_2^{\bullet -} + H^+ \leftrightarrow HO_2\cdot$	5.0×10^{10} $M^{-1}s^{-1}$ $k^-=7.9\times10^5$ $M^{-1}s^{-1}$	(Fathinia et al., 2016)
7	$2HO_2\cdot \rightarrow H_2O_2 + {}^1O_2$	5.0×10^9 $M^{-1}s^{-1}$	(Fathinia et al., 2016)
8	$O_3 + H_2O \xrightarrow{h\nu} H_2O_2$	—	(Lovato et al., 2009)
9	$O_3 + O_2^{\bullet -} \rightarrow O_3^{\bullet -} + O_2$	1.6×10^9 $M^{-1}s^{-1}$	(Lovato et al., 2009)
10	$O_3^{\bullet -} + H^+ \leftrightarrow HO_3\cdot$	5.2×10^{10} $M^{-1}s^{-1}$ $k^-=3.7\times10^4$ $M^{-1}s^{-1}$	(Fathinia et al., 2016)
11	$HO_3\cdot \rightarrow HO\cdot + O_2$	1.1×10^5 $M^{-1}s^{-1}$	(Fathinia et al., 2016)
12	$H_2O_2 + e^- \rightarrow HO\cdot + OH^-$	1.1×10^{10} $M^{-1}s^{-1}$	(Wang et al., 2018)

Table 2. Reactions involved in photocatalytic ozonation process at pH 7

Reaction No.	Reaction
13	$TiO_2/CDs + hv \rightarrow h^+ + e^-$
14	$TiO_2/CDs - H_2O + h^+ \rightarrow TiO_2/CDs - HO\cdot$
15	$TiO_2/CDs - OH^- + h^+ \rightarrow TiO_2/CDs - HO\cdot$
16	$TiO_2/CDs - e^- + O_3 \rightarrow TiO_2/CDs - O_3^{\bullet -}$
17	$TiO_2/CDs - e^- + O_2 \rightarrow TiO_2/CDs - O_2^{\bullet -}$
18	$TiO_2/CDs - O_2^{\bullet -} + O_3 \rightarrow TiO_2/CDs - O_3^{\bullet -}$
19	$TiO_2/CDs - O_3^{\bullet -} + H^+ \leftrightarrow TiO_2/CDs - HO_3\cdot$
20	$TiO_2/CDs - HO_3 \rightarrow HO\cdot + O_2$
21	$TiO_2/CDs - CIP + h^+ \rightarrow intermediates$
22	$TiO_2/CDs - CIP + HO\cdot \rightarrow intermediates$
23	$TiO_2/CDs - CIP + O_2^{\bullet -} \rightarrow intermediates$

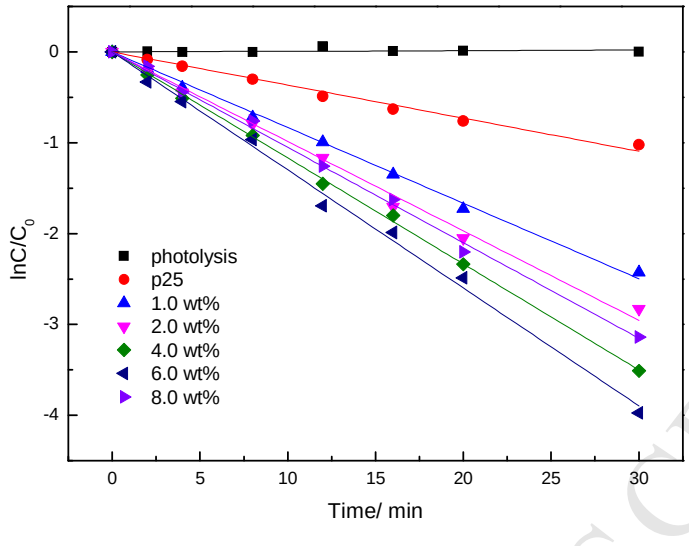

(a)

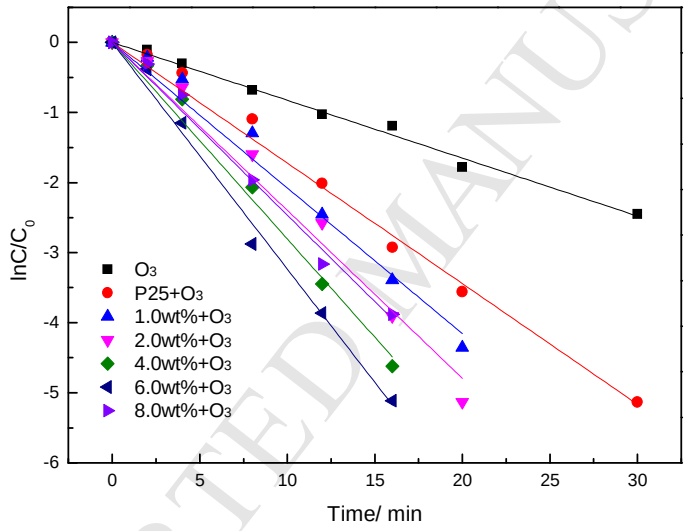

(b)

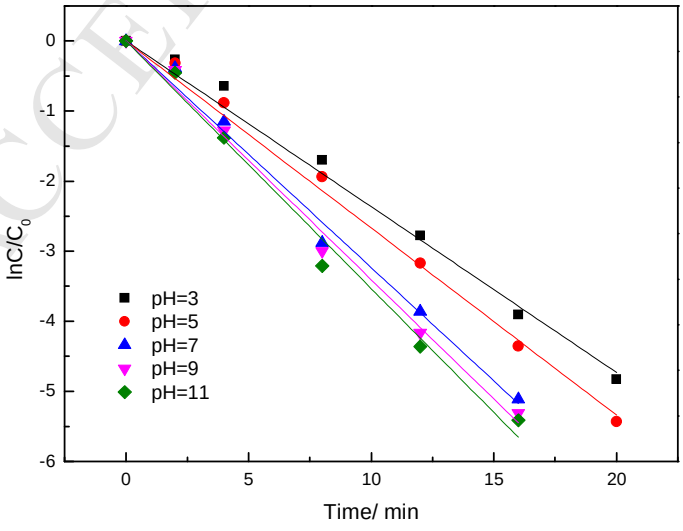

(c)

Fig.1(a) Degradation of CIP under simulated sunlight irradiation process over

CDs-TiO_2 with different CDs contents

(b) Degradation of CIP by photocatalytic ozonation process.

(c) Influence of initial pH on the degradation rate of CIP in photocatalytic ozonation process by 6 wt% TiO_2/CDs

Reaction conditions: $[CIP]_0$:10 ppm; catalysts loading : 6 wt% TiO_2/CDs 1g/L; ozone flow rate:15 mL/min; ozone concentration: 4.7 ppm; initial pH value: 7.0

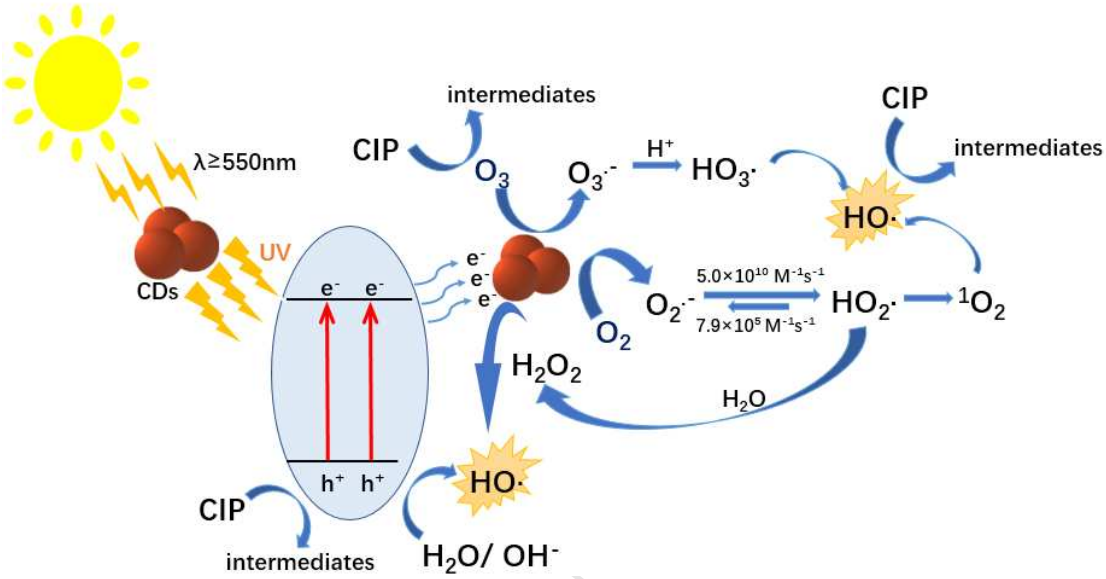

Fig.2 Proposed degradation mechanism of CIP by TiO_2/CDs and ozone under simulated sunlight irradiation

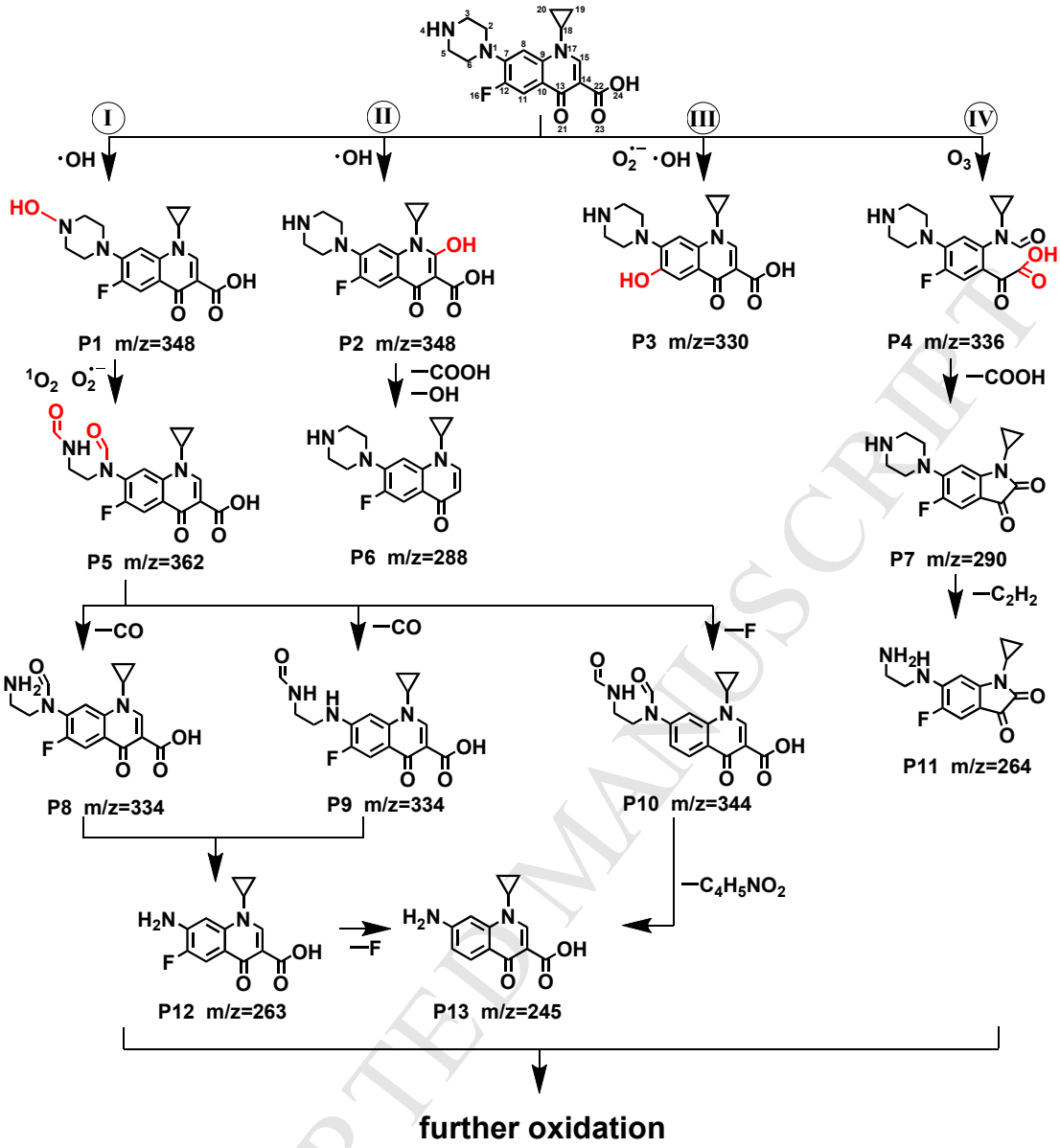

Fig.3 Possible transformation pathway of CIP in photocatalytic ozonation process

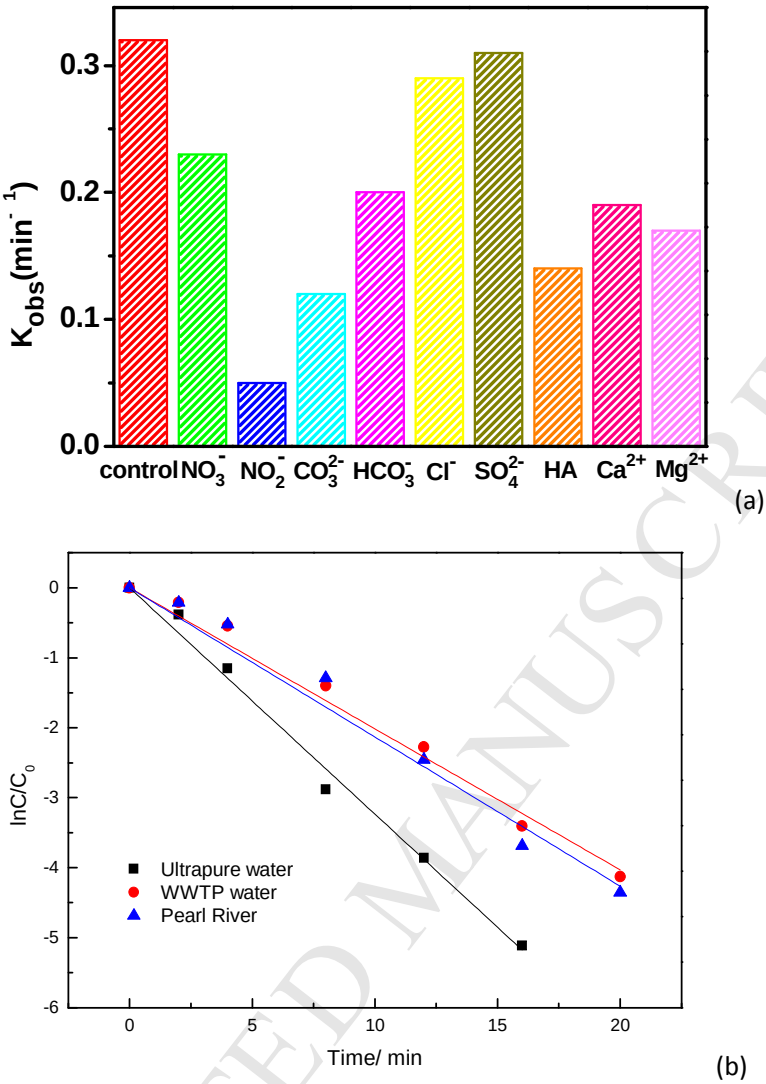

Fig.4 (a) Effect of different water constituents (b) effect of different water matrices on the degradation rate of CIP by 6 wt% TiO_2/CDs in photocatalytic ozonation process

•TiO_2/CDs exhibited extraordinary properties in photocatalysis and photocatalytic ozonation than pristine TiO_2.

•The function of CDs on TiO_2 showed well collaborated with ozone under sunlight irradiation.

•The enhanced activity in the process suggested participation of reactive species (•OH, $O_2^{\bullet-}$, h^+, etc.).

•The possible transformation pathway of CIP in photocatalytic ozonation process was proposed according to (HRAM) LC-MS/MS.